BJP British Journal of Pharmacology

DOI:10.1111/j.1476-5381.2010.01105.x
www.brjpharmacol.org

RESEARCH PAPER

# Phosphatidylinositol 3-kinase affects mitochondrial function in part through inducing peroxisome proliferator-activated receptor γ coactivator-1β expression

Minghui Gao, Junjian Wang*, Wenxian Wang†, Jinsong Liu and Chi-Wai Wong

*Guangzhou Institutes of Biomedicine and Health, Chinese Academy of Sciences, Guangzhou, China*

**Correspondence**
Chi-Wai Wong, Guangzhou Institute of Biomedicine and Health, Chinese Academy of Sciences, 190 Kai Yuan Avenue, Science Park, Guangzhou 510530, China. E-mail: wong_chiwai@gibh.ac.cn

Present addresses: *Room 1400 Research III Building, UC Davis Cancer Center/Basic Sciences, 4645 2nd Avenue, Sacramento, CA 95817, USA. †353 Biomedical Research Building, Oregon Health and Science University, 3181 Sam Jackson Road, Portland, OR 97239, USA.

Classification: Cancer pharmacology; Molecular & cellular mechanisms.

**Keywords**
mitochondrial function; PGC-1β; PI3K; ROS

**Received**
22 July 2010
**Revised**
29 September 2010
**Accepted**
14 October 2010

## BACKGROUND AND PURPOSE
Hyperactivation of phosphatidylinositol 3-kinase (PI3K), commonly observed in cancer, is believed to promote cancer cell growth and survival. Appropriate mitochondrial function is an integral part of cellular function. How PI3K affects mitochondrial homeostasis is not fully understood.

## EXPERIMENTAL APPROACH
Mitochondrial mass, membrane potential and reactive oxygen species (ROS) were quantified by three different fluorogenic probes. Gene expression at the levels of mRNA and protein were measured by quantitative RT-PCR and Western analysis.

## KEY RESULTS
Using the PI3K inhibitors LY294002 and PI103, we found that suppressing PI3K activity altered mitochondrial function. Specifically, LY294002 and PI103 suppressed the mRNA expression levels of mitochondrial regulators nuclear respiratory factors 1 and 2 (NRF1 and NRF2). As NRF1 and NRF2 are under the transcriptional control of peroxisome proliferator-activated receptor γ coactivators-1α and -1β (PGC-1α and PGC-1β), we found that suppressing PI3K activity selectively reduced both the mRNA and protein levels of PGC-1β but not PGC-1α. Reducing PGC-1β expression also led to reduced mRNA expression levels of uncoupling protein 1, 2 (UCP1 and UCP2) and superoxide dismutase 2. Correspondingly, mitochondrial membrane potential ($\Delta\psi_m$) and ROS levels were increased. Finally, we partially blunted the LY294002-mediated growth suppression by using an antioxidant or over-expressing PGC-1β.

## CONCLUSIONS AND IMPLICATIONS
PI3K regulates mitochondrial homeostasis in part through PGC-1β and blocking this pathway induces ROS to arrest cell growth at the $G_1$ phase.

## Abbreviations
$\Delta\psi_m$, mitochondrial membrane potential; ERRα and ERRγ, oestrogen-related receptor α and γ; MnTBAP, manganese(III) 5,10,15,20-tetrakis(4-benzoic acid)porphyrin; NRF1 and NRF2, nuclear respiratory factors 1 and 2; PDPK1, phosphoinositide dependent protein kinase 1; PGC-1α and PGC-1β, peroxisome proliferator-activated receptor γ

coactivators-1α and -1β; PI3K, phosphatidylinositol 3-kinase; PKB/Akt, protein kinase B; ROS, reactive oxygen species; SOD2, superoxide dismutase 2; Tfam, mitochondrial transcription factor A; UCP1 and UCP2, uncoupling proteins 1 and 2

## Introduction

Growth factor activation of receptor tyrosine kinase not only leads to the activation of mitogen-activated protein kinase kinase but also the phosphatidylinositol 3-kinase (PI3K) signalling pathway (Shaw and Cantley, 2006). As a lipid kinase, PI3K elevates the production of phosphoinositide-3,4,5-$P_3$, which activates phosphoinositide dependent protein kinase 1 (PDPK1). PDPK1 in turn phosphorylates and activates protein kinase B (PKB/Akt). The activated Akt then undergoes further auto-phosphorylation to fully initiate its activity and transmit the signal to multiple downstream targets including mammalian target of rapamycin. Protein and/or lipid phosphatases, such as tumour suppressor phosphatase and tensin homologue, act as negative regulators of this pathway. Dysregulation of this pathway, often in the form of amplifications of kinase expression, gain-of-function mutations in kinases and loss-of-function mutations in phosphatases, are frequently observed in a variety of tumours (Li *et al.*, 1997; Steck *et al.*, 1997; Samuels *et al.*, 2004; Bunney and Katan, 2010). Therefore, PI3K, Akt and mammalian target of rapamycin have emerged as important and attractive therapeutic targets for cancer and inhibitors of this pathway are currently being developed and tested in preclinical models and early phase clinical trials (Hennessy *et al.*, 2005; Liu *et al.*, 2009; Wong *et al.*, 2010).

Mitochondrial biogenesis is an important aspect of cellular function. Nuclear respiratory factors 1 and 2 (NRF1 and NRF2) directly regulate mitochondrial biogenesis by governing the expression of key components of the mitochondrial DNA transcription and replication machinery, as well as genes encoding respiratory subunits and the mitochondrial transport machinery (Scarpulla, 2008). These nuclear encoded mitochondrial transcription factors are themselves regulated at the transcriptional level by oestrogen-related receptor α and γ (ERRα and ERRγ) and their interacting cofactors such as peroxisome proliferator-activated receptor γ coactivator-1α and -1β (PGC-1α and PGC-1β) (Giguere, 2008; Villena and Kralli, 2008). ERRα, ERRγ, PGC-1α and PGC-1β promote mitochondrial biogenesis, regulate energy production and maintain redox homeostasis by binding to response elements located on the promoters and enhancers of their target genes such as mitochondrial transcription factor A (Tfam), uncoupling proteins (UCPs) and superoxide dismutases (SODs) (Giguere, 2008; Villena and Kralli, 2008).

Although the roles of PI3K in guiding cell growth and survival are more clearly defined, how PI3K affects mitochondrial homeostasis is not fully understood. Using PI3K inhibitors such as LY294002 and PI103, we found in this study that suppressing PI3K activity selectively reduced both the mRNA and protein levels of PGC-1β but not PGC-1α. Reducing PGC-1β expression led to reduced mitochondrial mass, elevated mitochondrial membrane potential ($\Delta\psi_m$), and induced the production of reactive oxygen species (ROS), which served to arrest cell growth at the $G_1$ phase. We have thus uncovered a mitochondrial homeostasis regulatory pathway involving PI3K and PGC-1β.

## Methods

### *Plasmids and chemicals*

A pGL3-PGC-1β promoter and an expression vector for full-length PGC-1β were cloned as previously described (Wang *et al.*, 2010b). LY294002 and PI103 were purchased from Cayman Chemical (Ann Arbor, MI, USA). Manganese(III) 5,10,15,20-tetrakis(4-benzoic acid)porphyrin (MnTBAP) was purchased from Calbiochem (San Diego, CA, USA). Drug/molecular target nomenclature conforms to the British Journal of Phamacology's Guide to Receptors and Channels (Alexander *et al.*, 2008).

### *Cell culture and cell growth assay*

Human lung adenocarcinoma A549 cells were purchased from American Type Culture Collection (ATCC, Manassas, VA, USA) and grown in RPMI-1640 medium (Gibco, Carlsbad, CA, USA) supplemented with 10% foetal bovine serum (HyClone, Guangzhou, China), 1× penicillin/streptomycin (Gibco, Carlsbad, CA, USA), and maintained at 37°C and 5% $CO_2$. Cell proliferation was quantified by trypan-blue exclusion assay. A549 cells were seeded into 24-well plates at $4 \times 10^4$ cells per well and cultured overnight followed by treatment with different doses of PI3K inhibitors for 48 h. Treated cells were washed twice with cold phosphate-buffered saline (PBS) and suspended in 300 μL PBS, then mix with 300 μL 0.4% trypan-blue solution (Sigma, CA, USA). Cell viability was determined by counting viable cells under a microscope by a haemacytometer.

### *Transfections*

Transient transfections were performed using Lipofectamine 2000 (Invitrogen, Carlsbad, CA, USA) following the manufacturer's instructions. For luciferase reporter assays, cells at 85–95% confluency in 96-well plates were cotransfected with reporter plasmids (25 ng per well) and *Renilla* luciferase (3 ng per well) as an internal control. Six hours after transfection, cells were treated with drugs for 24 h. Luciferase activity was measured as described previously (Xu *et al.*, 2010).

### *Cell cycle analysis*

As described previously (Wang *et al.*, 2010a), cells treated for 48 h with different doses of drugs were fixed with 70% ethanol, treated with 50 $\mu g \cdot mL^{-1}$ RNase A (Sigma, CA, USA), stained with 50 $\mu g \cdot mL^{-1}$ propidium iodide (Sigma, CA, USA) and analysed by flow cytometry for DNA synthesis and cell

cycle status (FACSCalibur instrument and CELLQUEST software, Becton Dickinson, CA, USA).

### Mitochondrial biogenesis assay

Mitotracker green (Invitrogen, Carlsbad, CA, USA) was added and quantified as described previously (Chen and Wong, 2009). Briefly, cells were incubated in serum-free medium (pre-warmed to 37°C) with 150 nM Mitotracker Green FM for 20 min in the dark. After being stained, the cells were washed twice with cold PBS and suspended in 200 μL PBS. Subsequently, cells were analysed on a FAC-SCalibur (BD Biosciences, San Jose, CA, USA) flow cytometer with excitation at 490 nm and emission at 516 nm. Data were processed by using the CellQuest program (BD Biosciences, San Jose, CA, USA).

### Reactive oxidant species assay

Reactive oxidant species production in mitochondria was measured by a cell-permeable fluorogenic probe MitoSOX Red (Invitrogen, Carlsbad, CA, USA) that is selectively targeted to the mitochondria, where it specifically reacts with superoxide anion as described previously (Liao *et al.*, 2010). Drug-treated cells were loaded with 5 μM MitoSOX Red for 10 min at 37°C, washed with PBS, and the fluorescence was detected with a flow cytometer (FAC-SCalibur, BD Biosciences, San Jose, CA, USA) with excitation at 510 nm and emission at 580 nm. Cellular peroxide level was determined based on the oxidation of 2,7-dichlorodihydrofluorescin (Beyotime, Jiangsu, China) as described by Wu *et al.* (2009). In brief, cells were washed and incubated with DCFH-DA for 20 min at 37°C in the dark. Cells were then washed twice and harvested in PBS. The fluorescence of 2,7-dichlorofluorescein was detected with a flow cytometer (FAC-SCalibur, BD Biosciences, San Jose, CA, USA) with excitation at 488 nm and emission at 530 nm. Data were processed by using a CellQuest programme (BD Biosciences, San Jose, CA, USA).

### Determination of $\Delta\psi_m$

The mitochondrial membrane potential was detected by using JC-1 dye (Beyotime, Jiangsu, China) as described by Nie and Wong (2009). Briefly, treated cells ($5 \times 10^5$ cells) were resuspended in 0.5 mL PBS and JC-1 was added at a final concentration of 1.0 μM. Samples were incubated for 15 min at 37°C. Green (~525 nm) and red (~590 nm) fluorescence were detected on a FACScan Becton–Dickinson flow cytometer (BD Facscalibur, Franklin Lakes, NJ, USA). The green fluorescence represents JC-1 monomers, whereas red fluorescence represents JC-1 aggregates.

### Quantitative real-time PCR

Total RNA extraction, first-strand cDNA generation and quantitative real-time PCR analysis were performed as described by Wang and Wong (2010). Relative gene expression was normalized to 18S rRNA levels. The primers used were as reported previously (Liao *et al.*, 2010; Wang *et al.*, 2010a,b).

### Western blot analysis

Cells were lysed using radio-immunoprecipitation assay reagent (Shenneng, Shanghai, China) according to the manufacturer's protocol and protein extracts were analysed by 10% sodium dodecyl sulphate polyacrylamide gel electrophoresis and blotted onto polyvinylidene fluoride membrane. Membranes were incubated with rabbit anti-human-ERRα, -ERRγ, -PGC-1α and -PGC-1β antibodies (Cell Signaling Technology, Boston, MA, USA), mouse anti-human-NRF1 antibody (Abcam, N.T., Hong Kong), rabbit anti-human-NRF2 antibody (Epitomics, CA, USA) or anti-β-actin antibody (Boster, Wuhan, China) followed by horseradish peroxidase-conjugated secondary antibody (Amersham, Piscataway, NJ, USA) and developed with BeyoECL Plus reagent (Beyotime, Jiangsu, China) as described by Wu *et al.* (2009).

### RNA interference

Small interfering RNA duplexes were designed by Ribobio (Guangzhou, China) and specific knockdown conditions were optimized using Lipofectamine 2000 (Invitrogen, Carlsbad, CA, USA). A final concentration of 50 nM of duplex was used to achieve knockdown as assessed by quantitative RT-PCR and Western blot analysis. siRNA duplexes at 50 and 100 nM were used to measure mitochondrial mass, mitochondrial membrane potential and peroxide levels. Target sequences for duplexes against human PGC-1β were 5′-GCGAGGUGCUGACAAGAAAdTdT-3′ and 5′-UUUCUU GUCAGCACCUCGCdTdT-3′.

### Statistical analysis

Assays done in triplicate were repeated at least three times. Data are presented as mean ± SE and were analysed by an analysis of variance (ANOVA) test.

## Results

### Suppressing PI3K activity reduces mitochondrial mass and arrests cell growth

As a downstream effector of PI3K, PDPK1 phosphorylates Akt at serine 473 to initiate the signal transduction process; thus, the extent of phosphorylation at serine 473 of Akt reflects the activity level of PI3K signalling pathway. By use of Western blot analysis, we first established that LY294002 effectively inhibited the activity of PI3K in A549 lung cancer cells (Figure 1A). LY294002 suppressed cell proliferation (Figure 1B) by arresting cells in the $G_1$ phase of the cell cycle but not by inducing cell death (Figure S1A–B). We then addressed if the LY294002-mediated growth suppression was correlated to mitochondrial biogenesis. The changes in mitochondrial mass were measured by staining the cells with Mitotracker Green, a dye that stains mitochondrion independent of its membrane potential. Confocal images of cells after staining with Mitotracker Green revealed that LY294002 generally reduced the total amount of mitochondrion per cell (Figure S1C). Upon quantitative measurement, we indeed found that LY294002 dose-dependently reduced mitochondrial mass (Figure 1C). In addition, we also found that LY294002 reduced mitochondrial mass in cervical cancer HeLa and another lung cancer cell line 95D (Figure S1D), indicating that this phenomena is applicable to other types of cancer cells. Because mitochondrial biogenesis is in part controlled by NRF1 and NRF2, we next examined the impact of LY294002 on the mRNA expression levels of these mitochon-

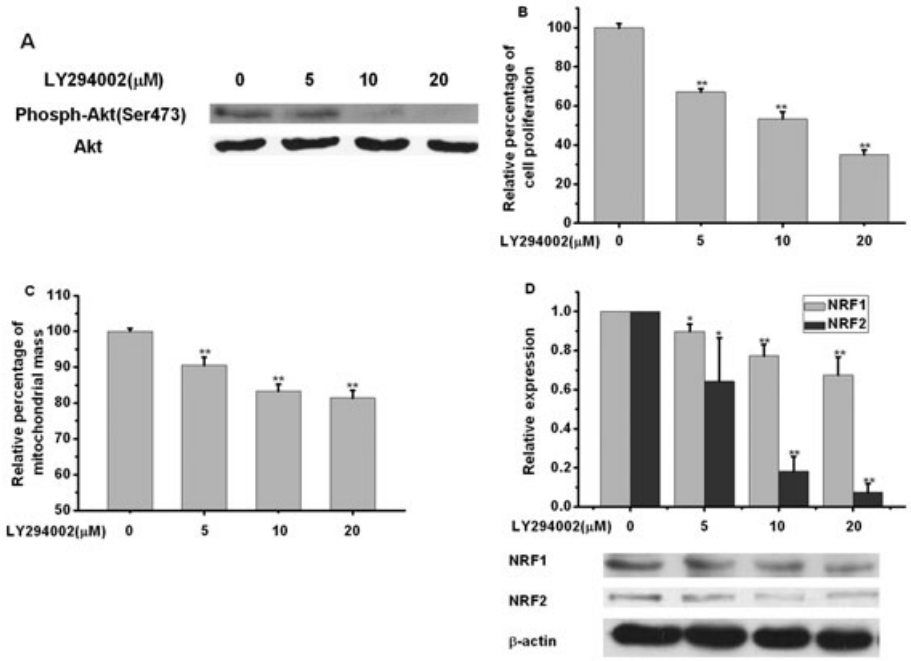


## Figure 1

LY294002 reduces mitochondrial mass and arrests cell growth. (A) Akt Ser 473 phosphorylation levels were analysed by Western blots using an antibody directed against phosphor-Akt with total Akt protein level as an internal control. (B) A549 cells were seeded into 24-well plates at a density of $4 \times 10^4$ cells per well. On the following day, different doses of LY294002 were added to the cells and incubated for another 48 h. The amount of cell growth in the presence of 0 μM LY294002 (dimethyl sulphoxide; DMSO as a control) was set as 100%. (C) A549 cells were seeded into 24-well plates at a density of $7 \times 10^4$ cells per well and cultured overnight. Mitochondrial mass of cells treated with LY294002 for 24 h were stained by Mitotracker™Green and quantified. The amount of mitochondrial mass in the presence of DMSO was set as 100%. (D) Gene expressions were detected using quantitative real-time PCR (qRT-PCR) and Western blots. NRFs were normalized to 18S rRNA and expressed as relative levels compared with DMSO. LY294002 compared with DMSO: $^*P < 0.05$; $^{**}P < 0.01$.

drial regulators. Consistent with the reduced mitochondrial mass, we found that both mRNA expression levels of NRF1 and NRF2 were dose-dependently suppressed by LY294002, with the suppression on NRF2 being more prominent (Figure 1D). Accordingly, the protein levels of NRF-1 and NRF-2 were also reduced (Figure 1D).

In addition, another PI3K inhibitor PI103 also dose-dependently suppressed cell proliferation (Figure 2A), arrested cells in the $G_1$ phase (Figure 2B), reduced mitochondrial mass (Figure 2C) and suppressed the expression levels of NRF1 and NRF2 (Figure 2D). Collectively, these data suggest that suppressing PI3K activity lowers NRF1 and NRF2 mRNA expression levels contributing to the reduction of mitochondrial mass, which correlates to growth suppression.

## *Suppressing PI3K activity elevates mitochondrial membrane potential and ROS production*

We next explored if suppressing PI3K activity altered mitochondrial function in addition to reducing mitochondrial mass. We used a fluorescent dye JC-1, which gives a red fluorescence when $\Delta\psi_m$ is high and green fluorescence when $\Delta\psi_m$ is low, to determine the overall electron transport chain activity. Indeed, confocal images and quantification measurements indicated that LY294002 dose-dependently increased the red fluorescence (Figure S1E–F). The red to green fluorescence ratio increased dose-dependently upon LY294002 treatment (Figure 3A), indicating an elevation in $\Delta\psi_m$. By allowing protons to pass through the mitochondrial membrane without coupling to ATP production, UCP1, 2 and 3 play essential roles in balancing $\Delta\psi_m$. We then investigated if the elevated $\Delta\psi_m$ was related to changes in UCP expressions. We found that the mRNA expression levels of UCP1 and UCP2 were selectively suppressed by LY294002, while the expression level of UCP3 remained relatively unchanged (Figure 3B).

An elevation in $\Delta\psi_m$ is consistent with a hyperactivated electron transport system in which excess electrons are passed to oxygen molecules to generate superoxide as ROS. A protection system against ROS is characterized by SOD1 and SOD2. We also checked the mRNA expression levels of SOD1 and SOD2 under the influence of LY294002 and found that it selectively suppressed the expression of SOD2, which resides in mitochondria (Figure 3C). The combined elevation in $\Delta\psi_m$ and reduction of SOD2 expression are likely to be the reasons behind the elevation in mitochondrial superoxide level detected using a specific probe MitoSox, shifting the distribution curve to the right (Figure S2). Because superoxide is readily converted to peroxide, we additionally measured the total cellular level of peroxide using another probe 2,7-dichlorodihydrofluorescin and found that LY294002

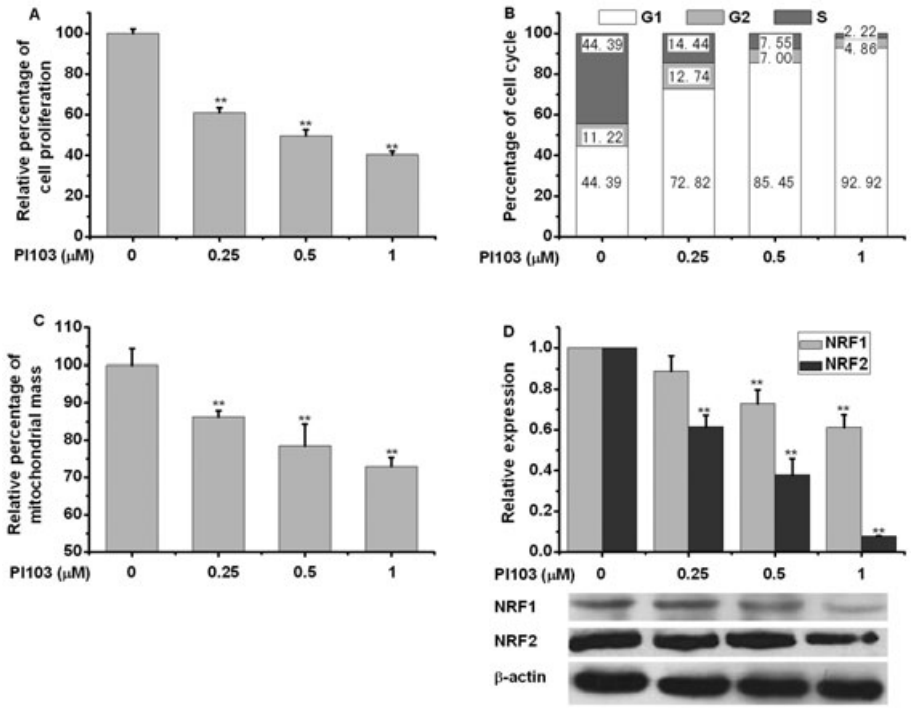


## Figure 2

PI103 reduces mitochondrial mass and arrests cell growth. (A) Cell proliferation was performed as in Figure 1 with different doses of PI103 indicated. (B) Cell cycle analysis was performed as in Methods. (C) Mitochondrial mass was measured as in Figure 1. (D) Gene expression was detected as in Figure 1. The effects of PI103 were compared with those of DMSO: $^{**}P < 0.01$.

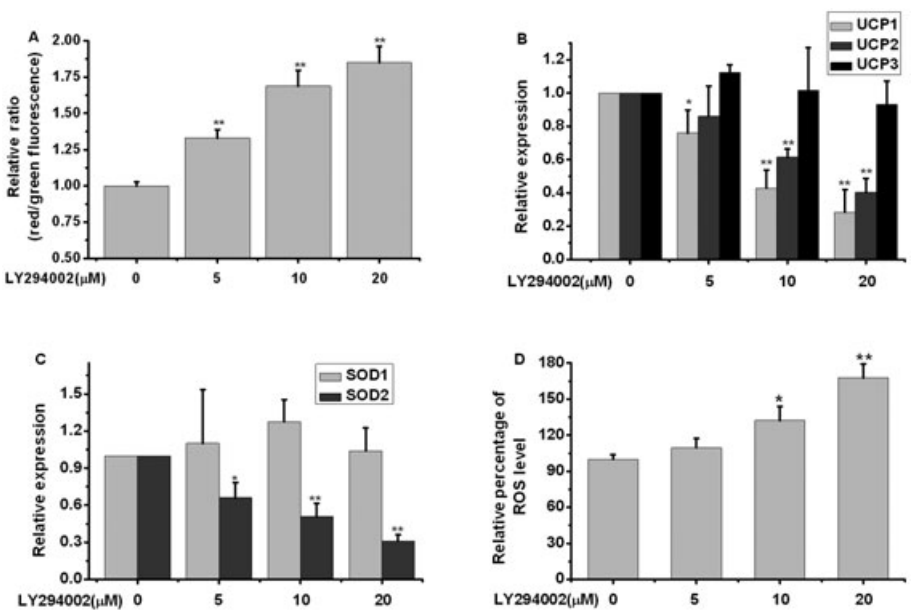


## Figure 3

Suppressing PI3K activity elevates mitochondrial membrane potential and reactive oxygen species (ROS) production. (A) Mitochondrial membrane potential was assayed by JC-1 staining and quantified by flow cytometry. The relative red to green ratio was expressed with reference to DMSO as a control. (B) UCPs expression levels were detected and expressed as in Figure 1D. (C) The expression levels of SOD1 and SOD2 were determined and expressed as in Figure 1D. (D) Effects of LY294002 on total cellular peroxide level were measured by a 2,7-dichlorodihydrofluorescin probe as described in Methods. (A–D) Results are expressed relative to level obtained with DMSO as a control. Effect of LY294002 compared with DMSO: $^{*}P < 0.05$; $^{**}P < 0.01$.

dose-dependently increased the peroxide level (Figure 3D). Similarly, suppressing PI3K activity by inhibitor PI103 also suppressed the expression levels of UCP1, UCP2 and SOD2 resulting in an elevated $\Delta\psi_m$ and ROS level (Figure S3A–E).

## *Suppressing PI3K activity selectively suppresses the expression of PGC-1β*

As ERRα, ERRγ, PGC-1α and PGC-1β play important roles in guiding the transcriptional expression levels of NRFs, UCPs and SODs, we checked the protein levels of these transcription factors and coactivators by Western blot analysis. We found that the protein levels of ERRα, ERRγ and PGC-1α were not significantly altered by LY294002 (Figure 4A). On the other hand, the protein level of PGC-1β was dramatically reduced (Figure 4A). To determine whether the suppression was at the transcriptional level, we measured the mRNA level of PGC-1β by quantitative RT-PCR analysis. We found that the mRNA expression level of PGC-1β was decreased after LY294002 treatment (Figure 4B). Additionally, the PI3K inhibitor PI103 also reduced the PGC-1β mRNA level (data not shown). We further demonstrated that the expression of a luciferase reporter under the control of PGC-1β promoter was dose-dependently reduced by LY294002 and PI103 (Figure 4C). As the altered mitochondrial homeostasis correlates with the reductions in PGC-1β at both the mRNA and protein levels, suppressing the expression of PGC-1β appears to be a primary event behind the LY294002-mediated effects.

## *Over-expression of PGC-1β partially reverses the alterations in mitochondrial function*

Because suppressing PI3K activity alters mitochondrial function leading to the accumulation of ROS, we next examined if this elevation of ROS level was important for the growth suppressive effect of LY294002. By using the antioxidant Mn(III) tetra(4-benzoic acid) porphyrin chloride (MnTBAP), which mimics the action of SOD to reduce the ROS level, we found that it partially reversed the growth suppressive effect of LY294002 (Figure 5A), indicating that ROS is an important cell cycle arrest mediator in these cancer cells. We then determined whether the down-regulation of PGC-1β expression by suppressing PI3K activity contributed to the alterations in mitochondrial function leading to ROS accumulation. We confirmed by Western blot analysis that PGC-1β was over-expressed through transient transfection of a PGC-1β expression plasmid (Figure 5B). This is consistent with PGC-1β playing a role in regulating mitochondrial function, over-expressing PGC-1β modestly reduced $\Delta\psi_m$ (Figure 5C) and ROS (Figure 5D) levels. Importantly, compared with a control plasmid, over-expressing PGC-1β partially blunted the LY294002-mediated elevations in $\Delta\psi_m$ (Figure 5C) and ROS (Figure 5D). Conversely, we attempted to reduce the expression level of PGC-1β by siRNA knockdown to see if it is sufficient to mimic the effects seen by inhibiting PI3K activity. An oligonucleotide was designed and confirmed to suppress PGC-1β expression at both the mRNA and protein levels (Figure 5E). Compared with a non-specific control, this PGC-1β siRNA dose-dependently reduced mitochondrial mass (Figure 5F). In addition, $\Delta\psi_m$ and ROS levels were dose-dependently elevated (Figure 5G–H). These changes are similar to those seen by LY294002 and PI103. Finally, another

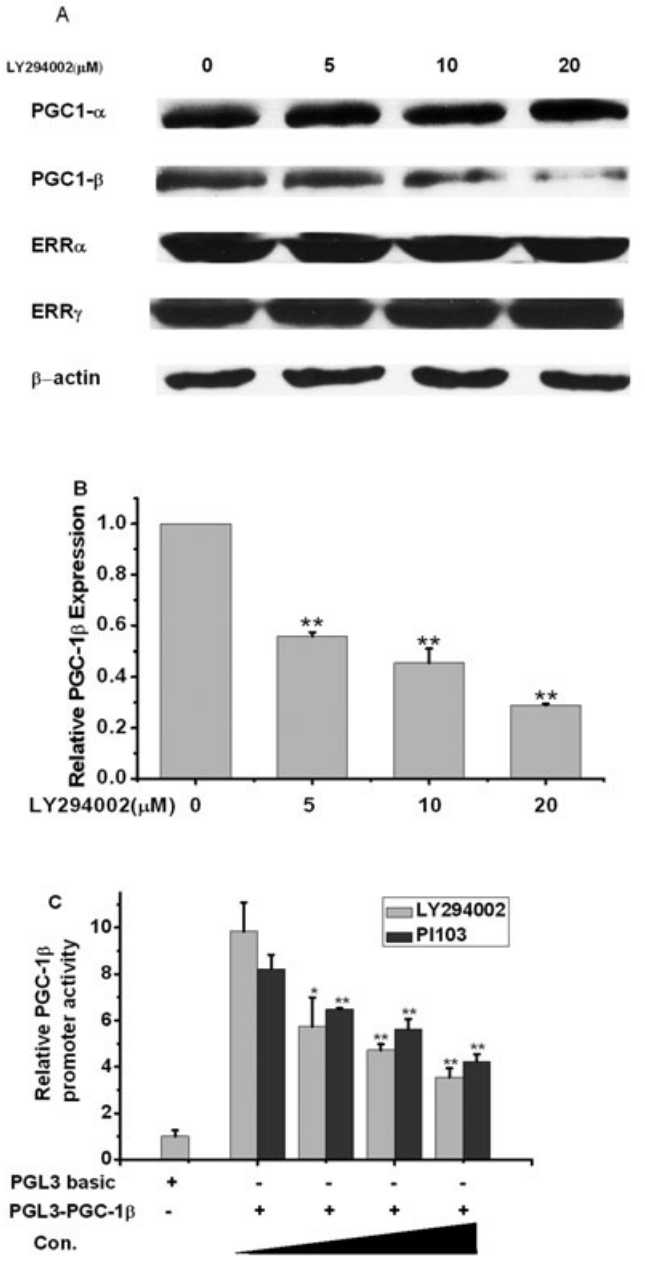


**Figure 4**

Suppressing PI3K activity selectively suppresses the expression of PGC-1β. (A) ERRs and PGC-1 s protein expression levels were assayed by Western blots with β-actin as an internal control. (B) PGC-1β gene expression levels were detected and expressed as in Figure 1D. (C) A549 cells were seeded into 96-well plates at $10^4$ cells per well, cultured overnight and then cotransfected with pGL3-basic control or pGL3-PGC-1β promoter with control *Renilla* luciferase plasmid. LY294002 or PI103 at 0, 5, 10 and 20 μM were added to the cells and incubated for another 24 h. Relative luciferase activity indicates the ratio of luciferase vs. *Renilla* activities. The effects of LY294002 or PI103 compared with DMSO: $^*P < 0.05$; $^{**}P < 0.01$.

PGC-1β siRNA oligonucleotide also reduced mitochondrial mass but elevated $\Delta\psi_m$ and ROS levels (Figure S4A–D). Collectively, these data strongly suggest that PGC-1β plays a part in guiding mitochondrial function under the influence of PI3K.

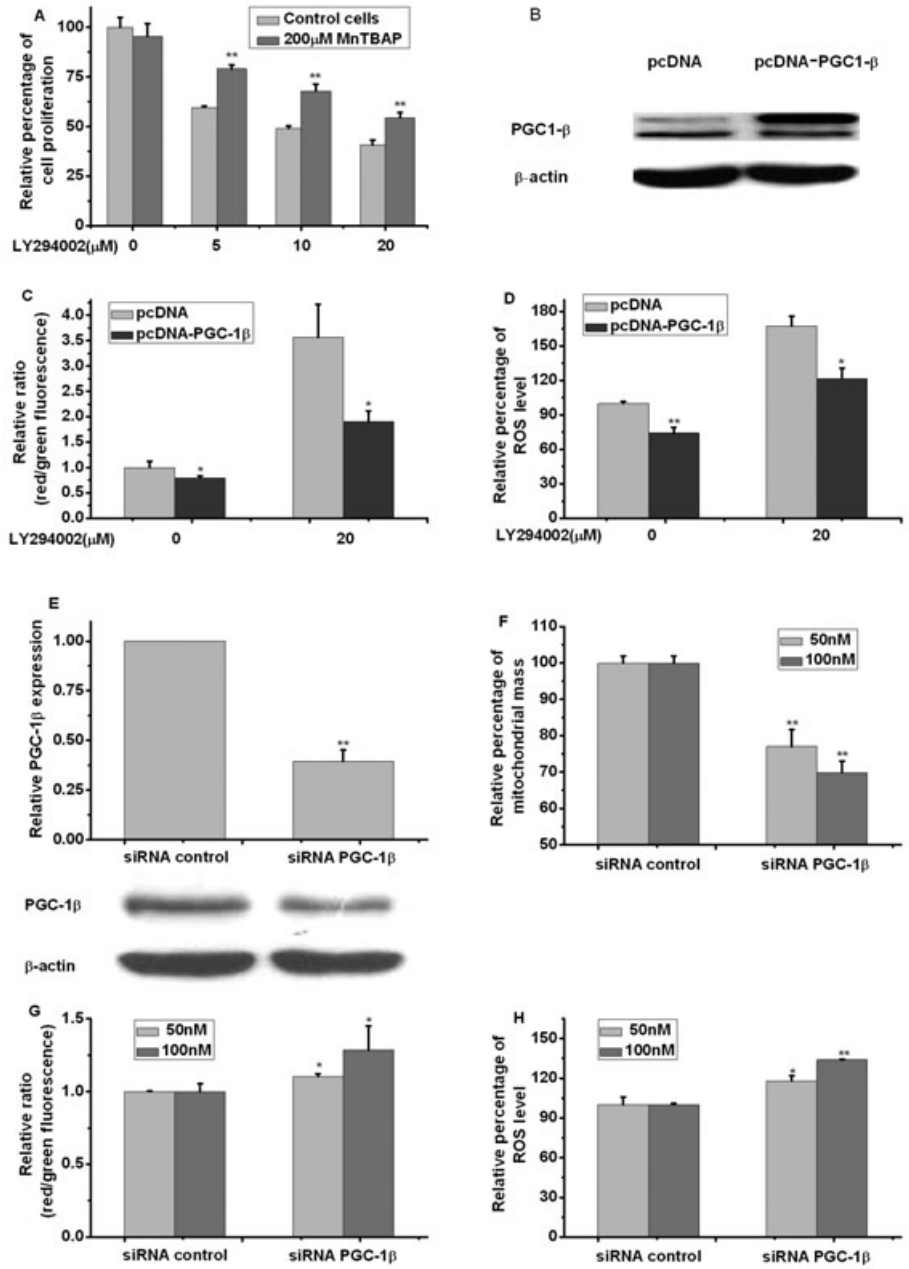


## Figure 5

Over-expression of PGC-1β partially reverses the alterations in mitochondria. (A) A549 cells were seeded into 96-well plates at $3 \times 10^3$ cells per well. On the following day, manganese(III) 5,10,15,20-tetrakis(4-benzoic acid)porphyrin (MnTBAP) was added to cells 2 h before the addition of DMSO or LY294002 for another 48 h before cell growth was determined as in Figure 1. MnTBAP compared with control cells: $^{**}P < 0.01$. (B) A549 cells were seeded into 6-well plates at $2 \times 10^5$ cells per well. On the following day, cells were transfected with 2 μg pcDNA or pcDNA-PGC-1β per well and incubated for 24 h. PGC-1β protein level was assayed by Western blots with β-actin protein as an internal control. (C–D) A549 cells were seeded into 24-well plates at $5 \times 10^4$ cells per well. On the following day, cells were transfected with 0.5 μg pcDNA or pcDNA-PGC-1β per well and incubated for 24 h. LY294002 was added to the cells and incubated for another 24 h. Mitochondrial membrane potential (C) and peroxide levels (D) were quantified and expressed as in Figure 2. PGC-1β over-expression compared with control: $^{*}P < 0.05$; $^{**}P < 0.01$. (E) PGC-1β expression after transfection of 50 nM of a non-specific oligonucleotide or PGC-1β siRNA. PGC-1β mRNA was detected by qRT-PCR, normalized to 18S rRNA and expressed as relative level compared with that obtained with a non-specific oligonucleotide as a control. PGC-1β Western blot analysis was compared with β-actin as a control. (F–H) Mitochondrial mass (F), $\Delta\psi_m$ (G) and ROS (H) levels were measured as in Figures 1 and 2 after dose-dependent transfection of non-specific or PGC-1β siRNA. PGC-1β siRNA compared with non-specific control: $^{*}P < 0.05$; $^{**}P < 0.01$.

## Discussion

PI3Ks are comprised of three different classes. Class I PI3K is a heterodimer of a regulator subunit (p85α, p55α, p50α, p85β or p55γ) and a catalytic subunit (p110α, p110β or p110δ). Among them, the gene encoding for the p110α subunit *PIK3CA* is frequently found to be mutated in human cancers (Samuels *et al.*, 2004), resulting in hyperactivation of its catalytic activity. Hyperactivation of PI3K pathway can also result from loss of function mutations in tumour suppressor phosphatase phosphatase and tensin homologue (Li *et al.*, 1997; Steck *et al.*, 1997). The importance of this pathway in guiding tumour development has been well recognized and inhibitors of PI3K are continuously being developed not just as anticancer therapeutics but also as pharmacological tools to help understand how the PI3K signalling pathway regulates diverse cellular function.

Proper mitochondrial function is an integral part of cell growth. Transcriptional coactivators PGC-1α, PGC-1β and their closely related member PGC-1-related coactivator govern numerous mitochondrial functions including mitochondrial biogenesis, oxidative phosphorylation, $\Delta\psi_m$ and an anti-ROS system (Handschin and Spiegelman, 2006). These coactivators function with their transcription factor partners such as ERRα, ERRγ, NRF1 and NRF2 to regulate the expression of their corresponding target genes. Whether PI3K regulates the expression or activity levels of this set of factors to affect mitochondrial homeostasis has hitherto not fully been investigated. Using PI3K inhibitors such as LY294002 and PI103 to suppress its activity, we demonstrated in this study that the mRNA and protein levels of PGC-1β were reduced. A loss of PGC-1β expression not only leads to a reduction of mitochondrial mass but also UCP1/2 and SOD2 expressions, which contribute to mitochondrial dysfunction characterized by elevations in Δψm and ROS levels. The increase in ROS serves to arrest cells at the $G_1$ phase. In other words, PI3K preferentially induces the expression of PGC-1β to affect mitochondrial homeostasis and cell cycle progression.

PGC-1α has been reported to play an important role in a protection system against ROS, specifically through regulating the expression of detoxifying enzymes like SOD1 and SOD2 that scavenge ROS (Wu *et al.*, 1999; St-Pierre *et al.*, 2006); whereas, we demonstrate here that suppressing PGC-1β expression also has an impact on this detoxification system. Noticeably, only the expression level of PGC-1β is regulated by the PI3K pathway. We attempted to probe into the mechanism responsible for this PI3K-directed PGC-1β expression. The expression of PGC-1β has been shown to be enhanced by ERRα (Arany *et al.*, 2007). We indeed found that the ERRα-induced enhancement of PGC-1β expression was suppressed by PI3K inhibitors (data not shown). This observation is consistent with the fact that ERRα activity is enhanced by activation of receptor tyrosine kinase, which acts upstream of PI3K (Barry and Giguere, 2005). Intriguingly, ERRα is a prognostic factor for breast, ovarian, prostate and colon cancers (Stein and McDonnell, 2006). Incidentally, using an ERRα specific inverse agonist XCT-790, we found that the expression level of PGC-1β was preferentially reduced in adipocytes (Nie and Wong, 2009). Collectively, these observations suggest that PI3K may enhance the activity of ERRα to induce PGC-1β expression and in such a manner regulates mitochondrial homeostasis to affect cell growth.

## Acknowledgements

This work was supported by grants from the One Hundred Person Project of the Chinese Academy of Sciences and the Knowledge Innovation Program of the Chinese Academy of Sciences (KSCX2-YW-R-084).

## Conflict of interest

The authors have nothing to declare.

## References

Alexander SPH, Mathie A, Peters JA (2008). Guide to Receptors and Channels (GRAC), 3rd edition. Br J Pharmacol 153: S1–S209.

Arany Z, Lebrasseur N, Morris C, Smith E, Yang W, Ma Y *et al.* (2007). The transcriptional coactivator PGC-1[beta] drives the formation of oxidative type IIX fibers in skeletal muscle. Cell Metab 5: 35–46.

Barry JB, Giguere V (2005). Epidermal growth factor-induced signaling in breast cancer cells results in selective target gene activation by orphan nuclear receptor estrogen-related receptor. Cancer Res 65: 6120–6129.

Bunney TD, Katan M (2010). Phosphoinositide signalling in cancer: beyond PI3K and PTEN. Nat Rev Cancer 10: 342–352.

Chen L, Wong C (2009). Estrogen-related receptor alpha inverse agonist enhances basal glucose uptake in myotubes through reactive oxygen species. Biol Pharm Bull 32: 1199–1203.

Giguere V (2008). Transcriptional Control of Energy Homeostasis by the Estrogen-Related Receptors. Endocr Rev 29: 677–696.

Handschin C, Spiegelman BM (2006). Peroxisome Proliferator-Activated Receptor Coactivator 1 Coactivators, Energy Homeostasis, and Metabolism. Endocr Rev 27: 728–735.

Hennessy BT, Smith DL, Ram PT, Lu Y, Mills GB (2005). Exploiting the PI3K/AKT Pathway for Cancer Drug Discovery. Nat Rev Drug Discov 4: 988–1004.

Li J, Yen C, Liaw D, Podsypanina K, Bose S, Wang SI *et al.* (1997). PTEN, a putative protein tyrosine phosphatase gene mutated in human brain, breast, and prostate cancer. Science 275: 1943–1947.

Liao X, Wang Y, Wong CW (2010). Troglitazone induces cytotoxicity in part by promoting the degradation of peroxisome proliferator-activated receptor gamma co-activator-1alpha protein. Br J Pharmacol 161: 771–781.

Liu P, Cheng H, Roberts TM, Zhao JJ (2009). Targeting the phosphoinositide 3-kinase pathway in cancer. Nat Rev Drug Discov 8: 627–644.

Nie Y, Wong C (2009). Suppressing the activity of ERRalpha in 3T3-L1 adipocytes reduces mitochondrial biogenesis but enhances glycolysis and basal glucose uptake. J Cell Mol Med 13: 3051–3060.

Samuels Y, Wang Z, Bardelli A, Silliman N, Ptak J, Szabo S *et al.* (2004). High frequency of mutations of the PIK3CA gene in human cancers. Science 304: 554.

Scarpulla RC (2008). Transcriptional paradigms in mammalian mitochondrial biogenesis and function. Physiol Rev 88: 611–638.

Shaw RJ, Cantley LC (2006). Ras, PI(3)K and mTOR signalling controls tumour cell growth. Nature 441: 424–430.

Steck PA, Pershouse MA, Jasser SA, Yung WK, Lin H, Ligon AH *et al.* (1997). Identification of a candidate tumour suppressor gene, MMAC1, at chromosome 10q23.3 that is mutated in multiple advanced cancers. Nat Genet 15: 356–362.

Stein RA, McDonnell DP (2006). Estrogen-related receptor alpha as a therapeutic target in cancer. Endocr Relat Cancer 13 (Suppl. 1): S25–S32.

St-Pierre J, Drori S, Uldry M, Silvaggi JM, Rhee J, Jager S *et al.* (2006). Suppression of Reactive Oxygen Species and Neurodegeneration by the PGC-1 Transcriptional Coactivators. Cell 127: 397–408.

Villena JA, Kralli A (2008). ERR[alpha]: a metabolic function for the oldest orphan. Trends Endocrinol Metab 19: 269–276.

Wang W, Wong CW (2010). Statins enhance peroxisome proliferator-activated receptor gamma coactivator-1alpha activity to regulate energy metabolism. J Mol Med 88: 309–317.

Wang J, Wang Y, Wong C (2010a). Oestrogen-related receptor alpha inverse agonist XCT-790 arrests A549 lung cancer cell population growth by inducing mitochondrial reactive oxygen species production. Cell Prolif 43: 103–113.

Wang Y, Fang F, Wong CW (2010b). Troglitazone is an estrogen-related receptor alpha and gamma inverse agonist. Biochem Pharmacol 80: 80–85.

Wong KK, Engelman JA, Cantley LC (2010). Targeting the PI3K signaling pathway in cancer. Curr Opin Genet Dev 20: 87–90.

Wu Z, Puigserver P, Andersson U, Zhang C, Adelmant G, Mootha V *et al.* (1999). Mechanisms Controlling Mitochondrial Biogenesis and Respiration through the Thermogenic Coactivator PGC-1. Cell 98: 115–124.

Wu F, Wang J, Wang Y, Kwok T-T, Kong S-K, Wong C (2009). Estrogen-related receptor [alpha] (ERR[alpha]) inverse agonist XCT-790 induces cell death in chemotherapeutic resistant cancer cells. Chem Biol Interact 181: 236–242.

Xu J, Liao X, Wong C (2010). Downregulations of B-cell lymphoma 2 and myeloid cell leukemia sequence 1 by microRNA 153 induce apoptosis in a glioblastoma cell line DBTRG-05MG. Int J Cancer 126: 1029–1035.

## Supporting information

Additional Supporting Information may be found in the online version of this article:

**Figure S1** (A) Cell cycle was analysed as described in Methods. (B) Cell death assays were performed by treating cells with either DMSO as a control, 100 nM doxorubicin, 20 μM LY294002 or 1 μM PI103 for 24 h. Cell death was detected by Annexin-V/7-amino-actinomycin D (7-AAD) staining. (C) Confocal images of cells after staining with Mitotracker Green with or without LY294002 or PI103 treatment. Briefly, cells were seeded onto coverslip in 6-well plates at a density of $2.5 \times 10^5$ per well and cultured overnight followed by treatments for 24 h. Cells were then incubated in serum-free medium (pre-warmed to 37°C) with 400 nM Mitotracker Green FM for 15 min in the dark. After being stained, cells were carefully washed twice with cold PBS and sections were taken with a Leica SP2 confocal microscope. (D) Mitochondrial mass of HeLa and 95D were measured after treating with LY294002 and expressed as a % of the values obtained with DMSO (0 μM LY294002) as a control. LY294002 compared with DMSO: **P*<0.05; ***P*<0.01. (E) Confocal images of cells after staining with JC-1 (red and green) and 4′,6-diamidino-2-phenylindole (DAPI) (blue) with or without LY294002 or PI103 treatment. As in (D) except 250 ng·mL$^{-1}$ DAPI and 2 μM JC-1 were used instead of Mitotracker Green. (F) Mitochondrial membrane potential revealed by JC-1 monomer vs. aggregates was shown for LY294002 treatments (red = PE and green = FITC).

**Figure S2** Effects of LY294002 on superoxide level, measured by MitoSox as described in Methods.

**Figure S3** (A) Akt Ser 473 phosphorylation levels were analysed by Western blots using an antibody directed against phosphor-Akt with total Akt protein level as an internal control. (B) Mitochondrial membrane potential after PI103 treatment shown as a ratio of that obtained in cells treated with DMSO. (C) UCPs expression levels were detected and expressed as in Figure 1D. (D) SODs expression levels of SOD1 and SOD2 were detected and expressed as in Figure 1D. (E) Peroxide levels were determined after addition of PI103. The effects of PI103 compared with those of DMSO: **P*<0.05; ***P*<0.01.

**Figure S4** (A) Another PGC-1β siRNA duplex (5′GAGC CGAAGUUGUACAGAAdTdT3′ and 5′UUCUGUACAACU UCGGCUCdTdT3′) was designed to knockdown its expression. PGC-1β expression was detected by qRT-PCR and Western blots. PGC-1β mRNA was normalized to 18S rRNA and expressed as relative levels compared with that obtained with a non-specific oligonucleotide as a control. (B–D) Mitochondrial mass (B), $\Delta\psi_m$ (C) and ROS (D) levels were measured as in Figure 5. PGC-1β siRNA compared with non-specific control: **P*<0.05.

Please note: Wiley-Blackwell are not responsible for the content or functionality of any supporting materials supplied by the authors. Any queries (other than missing material) should be directed to the corresponding author for the article.